OPEN ACCESS
JOURNAL OF ADVANCED DIELECTRICS
Vol. 13, No. 6 (2023) 2345001 (6 pages)

DOI: 10.1142/S2010135X23450017

XI'AN JIAOTONG UNIVERSITY

World Scientific
www.worldscientific.com

Out-of-plane photoconductive and bulk photovoltaic effects in two-dimensional α-In_2Se_3/Ta_2NiS_5 ferroelectric heterojunctions*

Dan Qiu, Jianing He, Shiwen Tan and Pengfei Hou†
School of Materials Science and Engineering, Xiangtan University
Hunan, Xiangtan 411105, P. R. China
†houpf@xtu.edu.cn

Received 22 May 2023; Revised 13 June 2023; Accepted 15 June 2023; Published 17 July 2023

Two-dimensional α-In_2Se_3 exhibits simultaneous intercorrelated in-plane and out-of-plane polarization, making it a highly promising material for use in memories, synapses, sensors, detectors, and optoelectronic devices. With its narrow bandgap, α-In_2Se_3 is particularly attractive for applications in photodetection. However, relatively little research has been conducted on the out-of-plane photoconductive and bulk photovoltaic effects in α-In_2Se_3. This limits the potential of α-In_2Se_3 in the device innovation and performance modification. Herein, we have developed an α-In_2Se_3-based heterojunction with a transparent electrode of two-dimensional Ta_2NiS_5. The out-of-plane electric field can effectively separate the photo-generated electron–hole pairs in the heterojunction, resulting in an out-of-plane responsivity (R), external quantum efficiency (EQE), and specific detectivity (D^*) of 0.78 mA/W, 10^{-3}% and 1.14×10^8 Jones, respectively. The out-of-plane bulk photovoltaic effect has been demonstrated by changes in the short circuit current (SCC) and open circuit voltage (V_{oc}) with different optical power intensity and temperature, which indicates that α-In_2Se_3-based heterojunctions has application potential in mid-far infrared light detection based on its out-of-plane photoconductive and bulk photovoltaic effects. Although the out-of-plane photoconductive and bulk photovoltaic effects are relatively lower than that of traditional materials, the findings pave the way for a better understanding of the out-of-plane characteristics of two-dimensional α-In_2Se_3 and related heterojunctions. Furthermore, the results highlight the application potential of α-In_2Se_3 in low-power device innovation and performance modification.

Keywords: Photoconductive effect; bulk photovoltaic effect; ferroelectric; heterojunction.

1. Introduction

Since the discovery of two-dimensional α-In_2Se_3 with simultaneous intercorrelated in-plane and out-of-plane polarization,[1–6] significant attention has been given to research on its properties. The attention is due to the excellent anisotropy, electrically and light-controlled polarization, and photoelectric effects that have been observed in this material.[7–12] These properties have shown potential for applications in memories, synapses, sensors, detectors, and optoelectronic devices.[13–20] Additionally, the layer-dependent narrow bandgap of two-dimensional α-In_2Se_3 makes it particularly attractive for use in photodetection.[21] Recent research has demonstrated that both in-plane and out-of-plane polarization can modulate the in-plane photodetection performance, which has reached a level comparable to that of commercial devices.[22] The α-In_2Se_3 has considerable in-plane anisotropic physical properties due to the different chain structures along the a and c axis. Compared to the in-plane photodetection properties, the out-of-plane photoconductive and bulk photovoltaic effects of two-dimensional α-In_2Se_3 have broader application prospects due to their ability to increase unit density.[23] This effect is helpful in developing detection modes and expanding detection wavelengths.[24–26] However, relatively little research has been conducted on the out-of-plane photoconductive and bulk photovoltaic in two-dimensional α-In_2Se_3, which limits the potential of two-dimensional α-In_2Se_3 in the device innovation and performance modification.

This report aims to investigate the out-of-plane photoconductive and bulk photovoltaic effects in two-dimensional α-In_2Se_3. To achieve this, a transparent electrode of two-dimensional Ta_2NiS_5 is introduced to form a two-dimensional α-In_2Se_3/Ta_2NiS_5 ferroelectric heterojunction. The results demonstrate that the electric field effectively separates the photo-generated electron–hole pairs out-of-plane in the heterojunction. The out-of-plane responsivity (R), external quantum efficiency (EQE), and specific detectivity (D^*) are approximately 0.78 mA/W, 10^{-3}% and 1.14×10^8 Jones, respectively. The out-of-plane bulk photovoltaic of the heterojunction is demonstrated by changes in the short circuit current (SCC) and open circuit voltage (V_{oc}) with different optical power intensity and temperature. This indicates that the α-In_2Se_3-based heterojunctions can convert light and thermal

*This paper was originally submitted to the Special Issue on Ferroelectric Nanoelectronic Devices for Next-Generation Information Technology organized by Zheng Wen, Shuoguo Yuan, Zhen Fan and Yunya Liu.

†Corresponding author.

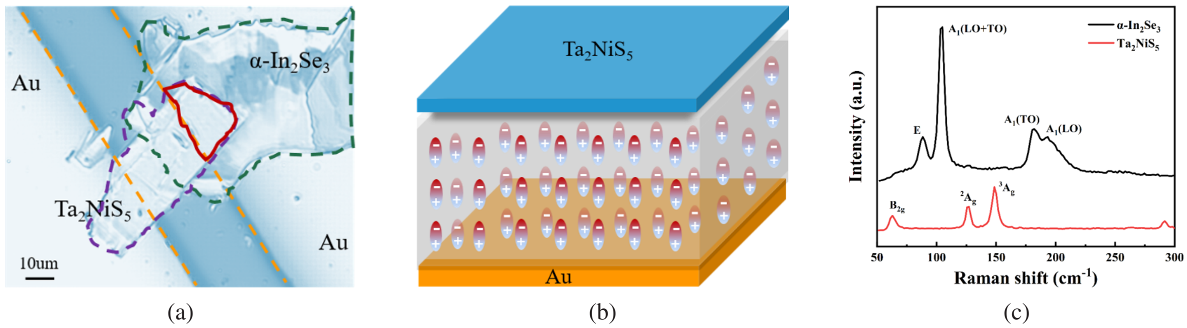

Fig. 1. Optical image (a), structure diagram (b) and Raman spectrum (c) of α-In_2Se_3/Ta_2NiS_5 ferroelectric heterojunctions, respectively.

energies in the surrounding environment into electrical energy, which can achieve self-powered photodetection and thermal detection. Although the out-of-plane photoconductive and bulk photovoltaic effects of α-In_2Se_3 are relatively lower than that of traditional materials, the findings in this study provide insight into the out-of-plane characteristics of two-dimensional α-In_2Se_3 and related heterojunctions. Additionally, the results highlight the application potential of α-In_2Se_3 in low-power device innovation and performance modification.

2. Experimental Methods

The structure in this work was formed by a few-layer α-In_2Se_3, Ta_2NiS_5 nanoflakes and two Au electrodes in the same horizontal space. The nanoflakes were obtained by mechanical exfoliation with the help of blue tape, the Au electrodes were deposited by a small ion sputtering instrument (SBC-12) using the mask with a channel width of 30 μm. To form the required heterojunction, the entire process was controlled by the two-dimensional transfer platform (E1-T) with the optical microscope (DMM-900C), which is a dry transfer technique. Subsequently, the flakes were sequentially transferred to the bottom electrode in the Si substrate with 300 nm SiO_2 layer on the surface by using polydimethylsiloxane (PDMS) film. It should be noted that the PDMS should be heated to 60°C–80°C about 10 min until the nanoflakes completely transferred to the substrate. This approach could connect two gold electrodes through α-In_2Se_3 and Ta_2NiS_5 thin films and ensure that there is an overlapping area between α-In_2Se_3 and Ta_2NiS_5 nanoflakes on one side of the gold electrode. Raman measurements of the fabricated devices were conducted via Renishaw inVia Raman microscopy with 532 nm laser excitation. The transmission electron microscopy (TEM) and selected area electron diffraction (SAED) images were investigated by transmission electron microscopy (JEM-2100). Finally, current–voltage (I_{ds}–V_{ds}) curves were measured by Agilent B1500A semiconductor device analyzer with a variable temperature probe station (EB8).

3. Results and Discussion

Figure 1(a) presents the optical image of a typical α-In_2Se_3/Ta_2NiS_5 ferroelectric heterojunction, where the section of Ta_2NiS_5, α-In_2Se_3 and Au electrode are marked with blue, green, and orange dotted lines, respectively, and the overlap area of these three is circled by the red line. Figure 1(b) reveals a capacitor-like structure where the ferroelectric material is sandwiched by the Ta_2NiS_5 and Au electrode. As Fig. 1(c) displayed, the Raman measurements of the α-In_2Se_3 reveal four pronounced peaks located at 88, 105, 182 and 193 cm^{-1}, respectively, agreement with the E, A_1(LO+TO), A_1(TO), and A_1(LO) vibration modes.[16,24] The three peaks of Ta_2NiS_5 nanoflakes located at 63, 127 and 149 cm^{-1} corresponding to atomic displacement modes for B_{2g}, ^2A_g, and ^3A_g, respectively.[27] In Fig. 2(a), a high-resolution TEM image clarifies that few-layer α-In_2Se_3 nanoflakes show a great crystallinity with a hexagonal lattice spacing of 0.35 nm corresponding to the (100) planes.[13] Figure 2(b) presents the TEM image of Ta_2NiS_5 single crystals, which can identify the crystalline interplanar spacing of 1.5 nm corresponding to the (001) planes close to the literature's results.[28] Two insets illustrate the SAED patterns of the nanoflakes, which show multiple sets of symmetry patterns and a perfect hexagonal structure of α-In_2Se_3 and Ta_2NiS_5.

As shown in Fig. 3(a), we measured the characteristic I_{ds}-V_{ds} curves of the α-In_2Se_3/Ta_2NiS_5 heterojunction under 660 nm laser with different power densities as bias within the range of ±3V. Figure 3(b) demonstrates the current density–voltage (J–V) curves of the α-In_2Se_3/Ta_2NiS_5 heterojunction, in which the tendency of curves is that the current

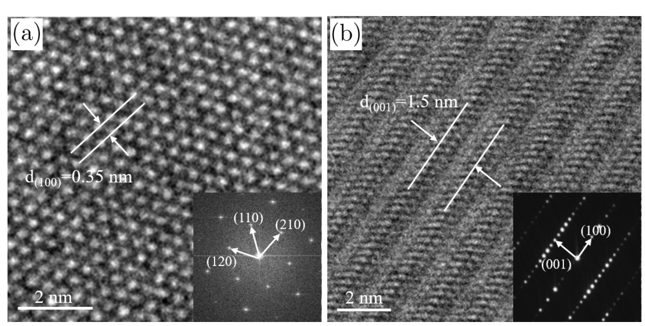

Fig. 2. The TEM images of α-In_2Se_3 (a) and Ta_2NiS_5 (b) nanoflakes, respectively. Insets illustrate the corresponding SAED patterns.

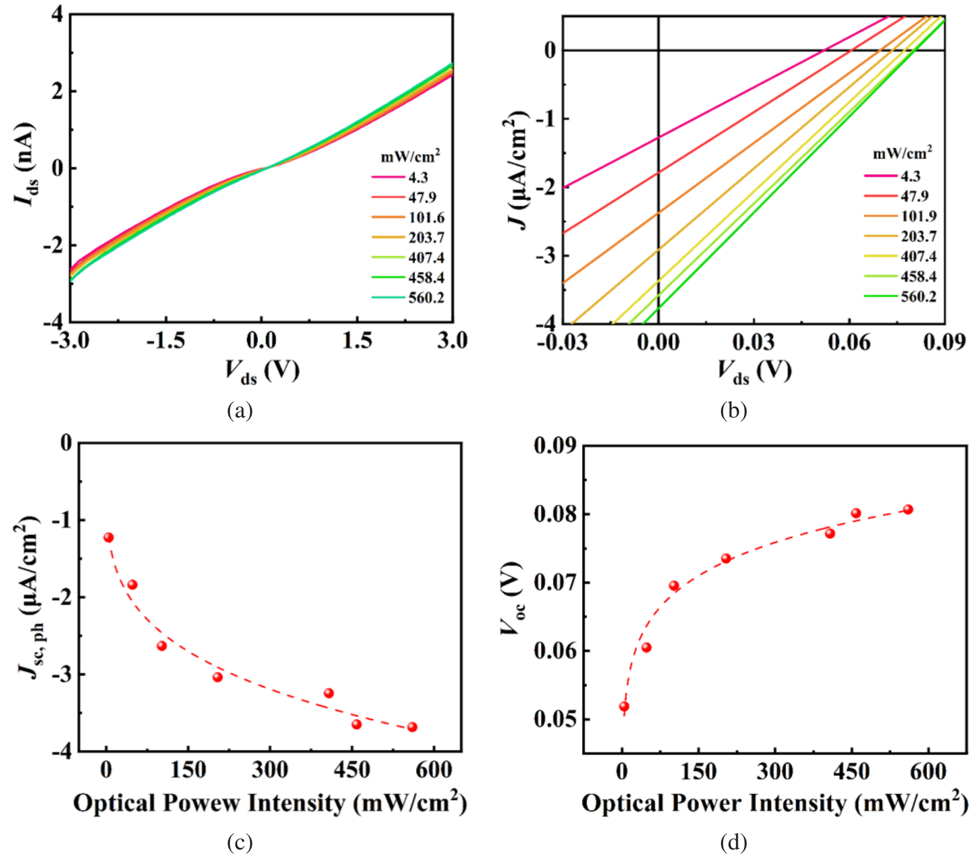

Fig. 3. Photoelectric effect in α-In_2Se_3/Ta_2NiS_5 ferroelectric heterojunctions. The characteristic output *I–V* curves (a) and *J–V* curves (b) of devices irradiated with laser (660 nm) in different optical power intensities. The $J_{sc,ph}$ (c) and V_{oc} (d) of the α-In_2Se_3/Ta_2NiS_5 heterojunction as functions of the optical power intensity.

density increases with the increase of optical power intensity. Although the out-of-plane direction photocurrent is relatively weak, it is still worth to attention. *SCC* density (J_{sc}) is equal to the *SCC* divided by the capacity area. Figures 3(c) and 3(d) show the value and tendency of the $J_{sc,ph}$ and V_{oc} of the α-In_2Se_3/Ta_2NiS_5 heterojunction in different power densities. When the laser is turned on, the increased negative $J_{sc,ph}$ could be observed without external bias. Both the $J_{sc,ph}$ and V_{oc} increase gradually with increasing laser power, which can be explained as the direction of the external bias voltage we applied is same to built-in electric field, which improves the separation efficiency of the electron–hole pairs, and then increases the out-of-plane photocurrent. The zero-bias photocurrent is thought to be a characteristic feature of bulk photovoltaic effect, which is a nonlinear optical process that converts light into electricity.[29,30] The electron–hole pairs are separated by a built-in electric field and collected by opposing electrodes, then producing *SCC* and V_{oc}. The maximum value of $J_{sc,ph}$ and V_{oc} is estimated to 3.68 μA/cm^2 and 0.08 V at the optical power intensity for 560.2 mW/cm^2, respectively.

To further investigate the origin of out-of-plane bulk photovoltaic effect and compare the contribution of light and heat to the current in α-In_2Se_3/Ta_2NiS_5 heterojunction, we measured I_{ds}-V_{ds} curves at different temperatures under dark condition, in which simulate the temperature varies caused by 660 nm laser. Figures 4(a) and 4(b) show the *J–V* curves when the temperature is heated up to 328 K from 298 K and cooled to 299 K from 328 K, respectively. Figures 4(c) and 4(d) show the changes of $J_{sc,py}$ and V_{oc} with temperature, whether heating or cooling, their trends increase gradually with the increase of temperature. According to the trend of fitting, the $J_{sc,py}$ and V_{oc} in the cooling process are slightly larger than that in the heating process. The inset explains temperature varies with the optical power intensity. The actual temperature corresponding to the optical power density of 560.2 mW/cm^2 is 311 K, where the $J_{sc,py}$ is about –1.53 μA/cm^2, the V_{oc} is about 0.06 V. By comparing Figs. 3 and 4, it is not difficult to find that the heat-induced $J_{sc,py}$ and V_{oc} is smaller than that generated by light, this is because the thermally induced polarization variation is relatively small, and the current is mainly generated by the separation of electron–hole pairs through the built-in electric field generated by the photovoltaic effect.

In addition, the photodetection performance of the α-In_2Se_3/Ta_2NiS_5 heterojunction is also investigated with a bias of 3 V. Figure 5(a) shows the changing curves of photocurrent (I_{ph}) with the optical power density increasing from

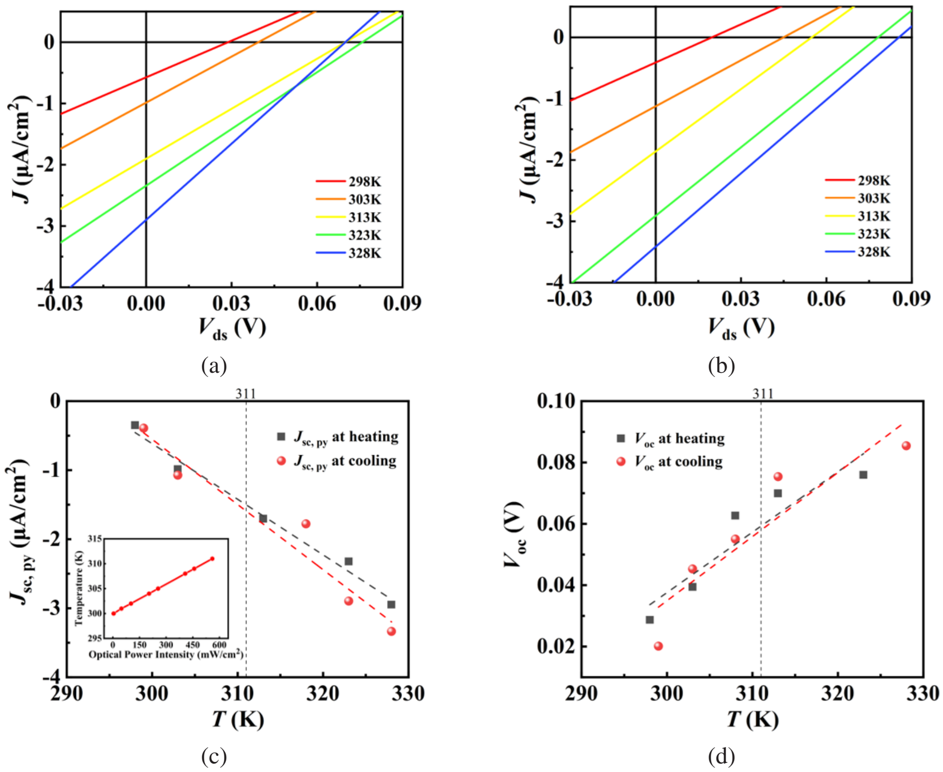

Fig. 4. The *J–V* curves of α-In_2Se_3/Ta_2NiS_5 heterojunction when temperature is rise (a) and down (b) at dark condition, respectively. The $J_{sc,py}$ (c) and V_{oc} (d) of the device change with temperature, inset shows the variation trend of temperature with optical power intensity.

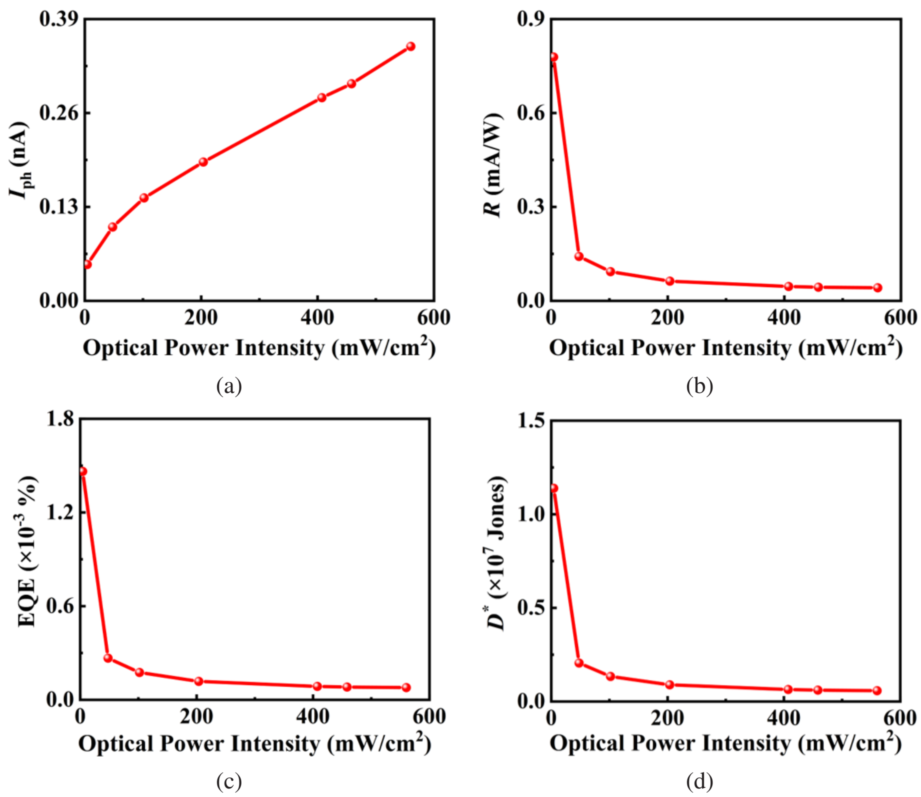

Fig. 5. Photodetection performance of α-In_2Se_3/Ta_2NiS_5 ferroelectric heterojunctions with a bias of 3 V. The I_{ph} (a), R (b), EQE (c) and D^* (d) as functions of optical power intensity, respectively.

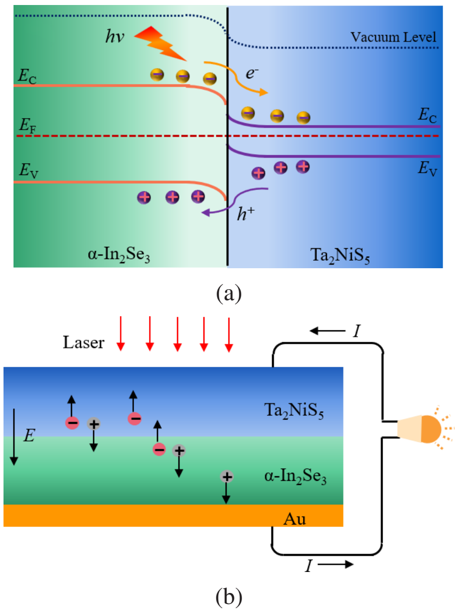

Fig. 6. The bandgap structure (a) and photovoltaic effect mechanism (b) of α-In_2Se_3/Ta_2NiS_5 heterojunctions under light condition.

0.05 nA at 4.3 mW/cm^2 to 0.35 nA at 560.2 mW/cm^2, which is small. The corresponding critical parameters, such as R, EQE and D^* are calculated by the following formulas: $R = I_{ph}/PS$, EQE = h$cR/e\lambda$, $D^* = R(S/2eI_{dark})^{1/2}$, where P is optical power intensity, S is the capacitance area formed, $\hbar$ is Planck's constant, c is the velocity of light, e is the elemental charge, λ is wavelength of incident light and I_{dark} is the current at dark environment.[31,32] As shown in Figures 5(b)–5(d), the value of R, EQE and D^* decrease with the increase of the optical power intensity, and the maximum value is 0.78 mA/W, 10^{-3}% and 1.14×10^8 Jones at the optical power intensity of 4.3 mW/cm^2, respectively. We find that the out-of-plane photodetection performance of the α-In_2Se_3/Ta_2NiS_5 heterojunction is relatively weak, which may due to the thin thickness of the α-In_2Se_3 nanoflakes. It can be concluded that the out-of-plane bulk photovoltaic effect of the α-In_2Se_3/Ta_2NiS_5 heterojunction is more promising in the application.

Figure 6(a) shows the bandgap structure of the device, when the α-In_2Se_3 and Ta_2NiS_5 construct a heterojunction, the charge will be redistributed to maintain the dynamic balance of diffusion carriers at the interface until the Fermi levels are aligned.[15] When the laser is turned on, the electrons near the valence band (E_V) transition to the conduction band (E_C),[27] the electron–hole pairs will be separated if they are produced within the space charge layer or if they can diffuse to it before recombining. This results in downward band bending for α-In_2Se_3 and upward band bending for Ta_2NiS_5, ultimately generating the photocurrent. Figure 6(b) illustrates the photovoltaic effect mechanism of α-In_2Se_3/Ta_2NiS_5 heterojunctions, photovoltaic effect is shown as the separation of photogenic electron–hole pairs through the polarization-induced internal electric field under the light, and the electrons and holes in the opposite direction drive and form photocurrent. When temperature changes, we noticed that the output photocurrent is variable although it is relatively weak. It indicates that the α-In_2Se_3/Ta_2NiS_5 heterojunction is sensitive to temperature, and the mid-far infrared light also cause temperature changes due to phonon vibration, so the device we fabricated also has a detection potential in mid-far infrared.

4. Summary

In this research, we have studied the out-of-plane photoconductive and bulk photovoltaic effects of the α-In_2Se_3/Ta_2NiS_5 ferroelectric heterojunction, the *SCC* and V_{oc} of the device change with different optical power intensity and temperature, which illustrates that the α-In_2Se_3-based heterojunction is a self-powered device and has certain application potential in the field of self-powered devices. The corresponding out-of-plane R, EQE, and D^* are approximately 0.78 mA/W, 10^{-3}% and 1.14×10^8 Jones at the optical power intensity for 4.3 mW/cm^2, respectively. Although the out-of-plane detection performance of the photodetector is relatively weak, the design of the α-In_2Se_3/Ta_2NiS_5 heterojunction provides a strategic approach to enhance and modulate photodetection performance, and the temperature of the device changed obviously under the light, which indicates the application potential in detecting mid-far infrared light based on the out-of-plane photoconductive and bulk photovoltaic effects.

Acknowledgments

This work was supported by the National Natural Science Foundation of China (No. 12175191), Natural Science Foundation of Hunan Province, China (Nos. 2022JJ30566), and the Research Foundation of Education Bureau of Hunan Province, China (Grant No. 22A0134).

Conflict of Interest

The authors have no conflicts to disclose.

Author Contributions

Dan Qiu and Jianing He contributed equally to this work.

References

[1] W. J. Ding, J. B. Zhu, Z. Wang, Y. F. Gao, D. Xiao, Y. Gu, Z. Y. Zhang and W. G. Zhu, Prediction of intrinsic two-dimensional ferroelectrics in In_2Se_3 and other III_2-VI_3 van der Waals materials, *Nat. Commun.* **8**, 14956 (2017).

[2] Y. Zhou, D. Wu, Y. H. Zhu, Y. J. Cho, Q. He, X. Yang, K. Herrera, Z. D. Chu, Y. Han and M. C. Downer, Out-of-plane piezoelectricity and ferroelectricity in layered α-In_2Se_3 nanoflakes, *Nano Lett.* **17**, 5508 (2017).

[3]Z. F. Liu, P. F. Hou, L. Z. Sun, E. Y. Tsymbal, J. Jiang and Q. Yang, In-plane ferroelectric tunnel junctions based on 2D α-In_2Se_3/ semiconductor heterostructures, *NPJ Comput. Mater.* **9**, 6 (2023).
[4]Z. Guan, H. Hu, X. W. Shen, P. H. Xiang, N. Zhong, J. H. Chu and C. G. Duan, Recent progress in two-dimensional ferroelectric materials, *Adv. Electron. Mater.* **6**, 1900818 (2020).
[5]P. F. Hou, S.W. Xing, X. Liu, C. Chen, X. L. Zhong, J. B. Wang and X. P. OuYang, Resistive switching behavior in α-In_2Se_3 nanoflakes modulated by ferroelectric polarization and interface defects, *Rsc. Adv.* **9**, 30565 (2019).
[6]P. F. Hou, C. L. Wang, Y. Chen, Q. Zhong, Y. K. Zhang, H. X. Guo, X. L. Zhong, J. B. Wang and X. P. Ou Yang, Ionization effect and displacement effect induced photoresponsivity degradation on α-In_2Se_3 based transistors for photodetectors, *Radiat. Phys. Chem.* **174**, 108969 (2020).
[7]M. Küpers, P. M. Konze, A. Meledin, J. Mayer, U. Englert, M. Wuttig and R, Dronskowski, Controlled crystal growth of Indium Selenide, In_2Se_3, and the crystal structures of α-In_2Se_3, *Inorg. Chem.* **57**, 11775 (2018).
[8]A. Xie, H. Hao, C. S. Liu, X. H. Zheng, L. Zhang and Z. Zeng, Giant tunnel electroresistance in two-dimensional ferroelectric tunnel junctions constructed with a Sc_2CO_2/In_2Se_3 van der Waals ferroelectric heterostructure, *Phys. Rev. B* **107**, 115427 (2023).
[9]P. F. Hou, Y. Lv, Y. Chen, Y. X. Liu, C. L. Wang, P. Zhou, X. L. Zhong, J. B. Wang and X. P. OuYang, In-plane strain-modulated photoresponsivity of the α-In_2Se_3-based flexible transistor, *ACS Appl. Electron. Mater.* **2**, 140 (2020).
[10]Z. Liu, J. Wu and J. B. Li, In-plane anisotropic electronic properties in layered α-In_2Se_3, *J. Appl. Phys*. **130**, 15103 (2021).
[11]C. L. Hsin, J. H. Huang, P. Spiewak, A. Ciupiński and S. W. Lee, Anisotropy of thermal conductivity in In_2Se_3 nanostructures, *Appl. Surf. Sci.* **494**, 867 (2019).
[12]G. H. Liu, K. X. Chen and J. T. Li, Combustion synthesis of InSe, In_2Se_3, and GaSe, *J. Am. Ceram. Soc.* **101**, 36 (2018).
[13]Y. X. Hu, W. Feng, M. J. Dai, H. H. Yang, X. S. Chen, G. B. Liu, S. C. Zhang and P. A. Hu, Temperature-dependent growth of few layer β-InSe and α-In_2Se_3 single crystals for optoelectronic device, *Semicond. Sci. Tech.* **33**, 125002 (2018).
[14]T. T. Guo, Z. X. Sa, P. F. Wei, Y. X. Jian, X. Chen, Z. S. Chen, J. Avila, P. Dudin, Z. X. Yang, X. F. Song, F. J. Liu and S. L. Zhang, High-performance flexible broadband photodetectors enabled by 2D Ta_2NiSe_5 nanosheets, *2D Materials* **10**, 025004 (2023).
[15]D. Dutta, S. Mukherjee, M. Uzhansky, P. K. Mohapatra, A. Ismach and E. Koren, Edge-based two-dimensional α-In_2Se_3-MoS_2 ferroelectric field effect device, *ACS Appl. Mater. Interfaces* **15**, 18505 (2023).
[16]C. Jia, S. X. Wu, J. Z. Fan, C. J. Luo, M. H. Fan, M. Li, L. P. He, Y. J. Yang and H. Zhang, Ferroelectrically modulated and enhanced photoresponse in a self-powered α-In_2Se_3/Si heterojunction photodetector, *ACS Nano* **17**, 6534 (2023).
[17]J. J. Zha, S. H. Shi, A. Chaturvedi, H. X. Huang, P. Yang, Y. Yao, S. Y. Li, Y. P. Xia, Z. M. Zhang, W. Wang *et al*., Electronic/optoelectronic memory device enabled by tellurium-based 2D van der Waals heterostructure for in-sensor reservoir computing at the optical communication band, *Adv. Mater* **35**, 2211598 (2023).
[18]S. Y. Wan, Q. Peng, Z. Y. Wu and Y. B. Zhou, Nonvolatile ferroelectric memory with lateral $\beta/\alpha/\beta$ In_2Se_3 heterojunctions, *ACS Appl. Mater. Interfaces* **14**, 256930 (2022).
[19]X. Tang, J. Shang, Y. D. Ma, Y. T. Gu, C. F. Chen and L. Z. Kou, Tuning magnetism of metal porphyrazine molecules by a ferroelectric In_2Se_3 monolayer, *ACS Appl. Mater. Interfaces* **12**, 39561 (2020).
[20]L. H. Jin, H. D. Wang, R. Cao, K. Khan, A. K. Tareen, S. Wageh, A. A. Al-Ghamdi, S. J. Li, D. B. Li, Y. Zhang and H. Zhang, The rise of 2D materials/ferroelectrics for next generation photonics and optoelectronics devices, *Apl Mater.* **10**, 60903 (2022).
[21]J. X. Zhang, X. L. Zhang, Y. Wang, P. Cheng, B. J. Feng, K. H. Wu, Y. H. Lu and L. Chen, Giant bandgap engineering in two-dimensional ferroelectric α-In_2Se_3, *J. Phys. Chem. Lett.* **13**, 3261 (2022).
[22]J. Igo, M. Gabel, Z. G. Yu, L. L. Yang and Y. Gu, Photodefined in-plane heterostructures in two-dimensional In_2Se_3 nanolayers for ultrathin photodiodes, *ACS Appl. Nano Mater.* **2**, 6774 (2019).
[23]T. Yan, F. J. Liu, Y. R. Wang, J. Yang, C. Y. Ding, Y. C. Cai, Z. L. Wu, X. Y. Zhan, F. Wang, Y. H. Tian, J. He and Z. X. Wang, A ferroelectric p-i-n heterostructure for highly enhanced short-circuit current density and self-powered photodetection, *Adv. Electron. Mater.* **8**, 2101385 (2022).
[24]H. Z. Li, K. Zhang, X. Li, B. Q. Liu, L. B. Li, Z. X. Mei, T. S. Chen, Q. Z. Liu, W. Z. Yu, J. Yuan, H. R. Mu and S. H. Lin, Two-dimensional (2D) α-In_2Se_3/Ta_2NiSe_5 heterojunction photodetector with high sensitivity and fast response in a wide spectral range, *Mater Design* **227**, 111799 (2023).
[25]X. W. Guan, X. C. Yu, D. Periyanagounder, M. R. Benzigar, J. K. Huang, C. H. Lin, J. Y. Kim, S. Singh, L. Hu, G. Z. Liu, D. H. Li, J. H. He, F. Yan, Q. J. Wang and T. Wu, Recent progress in short- to long-wave infrared photodetection using 2D materials and heterostructures, *Adv. Opt. Mater.* **9**, 2001708 (2021).
[26]I. C. Paul, R. J. Mathew, R. Sankar, H. Y. Lin, N. X. Li, Y. T. Chen and Y. F. Chen, Coupling between pyroelectricity and built-in electric field enabled highly sensitive infrared phototransistor based on InSe/WSe(2)/P(VDF-TrFE) heterostructure, *ACS Appl. Mater. Interfaces* **15**, 19121 (2023).
[27]X. H. Meng *et al*., Giant superlinear power dependence of photocurrent based on layered Ta_2NiS_5 photodetector, *Adv. Sci.* 2300413 (2023).
[28]L. Li, P. L. Gong, W. K. Wang, B. Deng, L. J. Pi, J. Yu, X. Zhou, X. Q. Shi, H. Q. Li and T. Y. Zhai, Strong in-plane anisotropies of optical and electrical response in layered dimetal chalcogenide, *ACS Nano* **11**, 10264 (2017).
[29]Y. H. Zeng, F. X. Meng, S. D. Fan, P. F. Wang, C. Y. Kou, M. Y. Sun, H. G. Hu, R. Cao, S. Wageh, O. A. Al-Hartomy, A. Kalam, B. W. Du, W. C. Ding, S. R. Wei, Z. N. Guo, Q. L. Wang and H. Zhang, Fully depleted vdW heterojunction based high performance photovoltaic photodetector, *J. Materiomics* 2352 (2023).
[30]Y. Li, J. Fu, X. Y. Mao, C. Chen, H. Liu, M. Gong and H. L. Zeng, Enhanced bulk photovoltaic effect in two-dimensional ferroelectric $CuInP_2S_6$, *Nat. Commun.* **12**, 5896 (2021).
[31]J. T. Yuan, S. T. Zhou, B. H. Xiao, L. J. Bao, Z. K. Ai, Y. H. Shen, G. Ran and Q. J. Cheng, Monolayer WS_2 nanosheets passivated with HfO_2 for enhanced photodetectors, *ACS Appl. Nano Mater.* **6**, 4594 (2023).
[32]J. J. Hei, X. Li, S. E. Wu, P. Lin, Z. F. Shi, Y. T. Tian, X. J. Li, L. H. Zeng, X. C. Yu and D. Wu, Wafer-scale patterning synthesis of two-dimensional WSe_2 layers by direct selenization for highly sensitive van der Waals heterojunction broadband photodetectors, *ACS Appl. Mater. Interfaces* **15**, 12052 (2023).